High performance piezoresitive response of nanostructured ZnO/Ag thin films for pressure sensing applications

Armando Ferreira[a,*], João Paulo Silva[a], Rui Rodrigues[a], Nicolas Martin[b], Senentxu Lanceros-Méndez[c,d], Filipe Vaz[a]

[a]Centro de Física, Universidade do Minho, 4710-057 Braga, Portugal

[b]Institut FEMTO-ST, UMR 6174 CNRS, Univ. Bourgogne Franche-Comté, 15B Avenue des Montboucons, 25030 Besançon Cedex, France

[c]BCMaterials, Basque Center for Materials, Applications and Nanostructures, UPV/EHU Science Park, 48940 Leioa, Spain

[d]IKERBASQUE, Basque Foundation for Science, 48013 Bilbao, Spain

[*]Corresponding author: armando.f@fisica.uminho.pt; tel: +361 253 510 475, fax: +351 253 601 059

Highlights

- ZnO/Ag thin films were prepared by GLancing Angle Deposition.

-

- Ag content and zigzag architecture contribute to the piezoresisisve response.

- Gauge Factor values up to 120 ± 3 are obtained.

-Gauge facture is correlated to the conductive tunneling distance, ranging from 0.1 to 10 nm.

Abstract

This work reports on the preparation and characterization of zigzag nanostructured Silver (Ag) doped Zinc Oxide (ZnO) in order to improve piezoresistive response for pressure sensor applications. ZnO/Ag thin films were prepared by Glancing Angle Deposition (GLAD), sputtered from a metallic Zinc (Zn) target. The target was customized with different amounts of Ag pellets, symmetrically distributed along the preferential erosion area.

It is shown that increasing the Ag content in the ZnO/Ag system leads to a decrease of the electrical resistivity from 2.95 Ω.cm to 1.52×10^{-5} Ω.cm. The structural characterization of the thin films shows an evolution of the preferential growth, changing from a polycrystalline ZnO hexagonal-like structure, confirmed by the presence of dominant ZnO (002) and ZnO (101) diffraction peaks, to a Ag cubic (fcc)-like structure, as evidenced by the Ag (111), (200) and (220) diffraction peaks. The values of the gauge factor show a strong contribution both from Ag as well as from the zigzag nanostructure to the piezoresistive sensitivity of the films, in particular for Ag concentrations lower than 66 at.%. The tunneling distance was calculated for the different samples and in three different deformation regions, in order to evaluate the influence the distance between pairs of Ag conductive nanoregions on the piezoresistive sensitivity. The results show that a longer distance between Ag particles, which varies from 0.1 to 10 nm, leads to enhanced GF, which ranges from 8 ± 1 to 120 ± 3, respectively.

Keywords: Sensors; Zinc Oxide; Silver; Gauge Factor; DC Magnetron Sputtering; Electromechanical properties.

1. Introduction

Piezoresistive strain sensors react to mechanical deformations by the change of resistance. Several criteria characterize high-performance strain sensors, including sensitivity (i.e., higher gauge factor, GF), stretchabilty, response time, fabrication cost, and stability. Recently, it has been numerous efforts to develop flexible, stretchable, and highly sensitive strain sensors due to their wide application areas, including rehabilitation and personal health monitoring [1], wearable electronics devices, such as artificial e-skins [2] or robotic skins [3], among others. For this purpose, several types of flexible and stretchable sensors were proposed through the combination of carbon nanotubes and polymers as the support materials, revealing excellent electrical and mechanical properties [4–6].

By contrast, the relationship between mechanical and electrical behavior becomes even more important if the proposed systems are prepared in the form of thin films, since their strain sensitivity is expected to be different from those of the bulk materials, due to size effects and the increased relevance of micro and nanostructural features. Some reports proved that the doping an insulator matrix with one or more different metals, including Ag, Au, or Cu, to construct a conductive network [7,8], might be interesting candidates for these kind of applications. Generally, these works were dedicated to evaluate the conductivity and critical metal filler fraction, at which a system exhibits a transition from insulating to conductive behavior, typically explained within the framework of the percolation theory [9,10]. However, very little works have been focused on the sensing properties of these systems [7,11–13]. Additionally, an emerging and attractive method to fabricate strain sensing materials is being developed [14], aiming at the development of material systems where the electrode material itself acts as a sensor. This is particularly challenging given the relatively high and complex mechanical solicitations that are expected in several of these applications, i.e., bending, elongation and torsion. In the literature, the most explored solutions use silver as conductive

filler, based on indium tin oxide, ITO/Ag [15] and indium zinc oxide, IZO/Ag [16]. However, indium-free Zinc Oxide, ZnO, -based are preferable to ITO because of the cost factor, and ZnO is known to be an excellent seed layer for the growth of Ag [17].

The present work demonstrates a new approach, based on the optimization of nanostructured zigzag-like ZnO/Ag thin films with different amounts of Ag deposited on flexible polymeric PET - Polyethylene terephthalate by *GLancing Angle Deposition* (GLAD) [18], for the development of piezoresistive thin film sensors. It is shown that the optimized thin films can be used as flexible and stretchable piezoresistive strain sensors.

2. Experimental details

ZnO/Ag thin films were DC sputtered from a metallic zinc (Zn) target (with dimensions 20×10×0.6 cm^3 and 99.96 at.% purity), using a custom-made vacuum chamber. The Zn target was customized with different amounts of Ag pellets (with individual area of ~ 0.2 cm^2), symmetrically distributed along the preferential erosion area, Fig. 1a), in order to tune the silver content in the coatings.

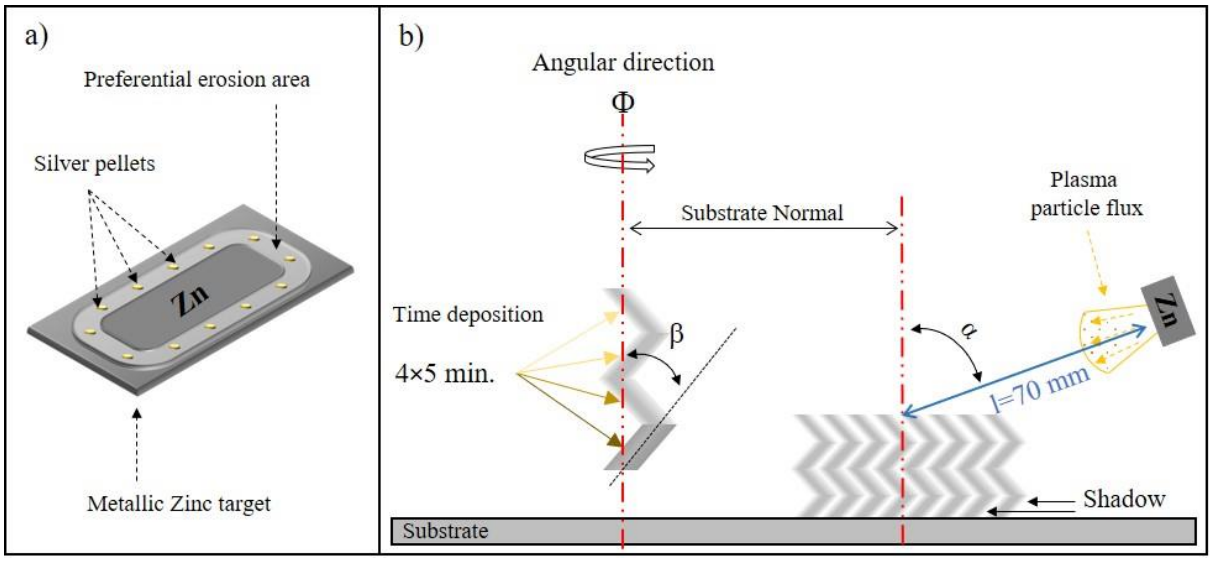

Figure 1. a) Schematic representation of the distribution of the Ag pellets on the Zn target and **b)** of the GLAD system, where Φ is the angular direction, α is the incidence angle of the Zn particle flux and β is the columnar growth angle,

The incidence angle of the Zn particle flux (α) was determined from the substrate normal, by tilting the substrate holder at 45º [13]. The Zn target was sputtered during 20 min, 4×5 min for each component of the zigzag structure, Fig.1 b), with a constant argon flow rate of 25 sccm (total pressure of 0.28 Pa). Oxygen was added in the gas atmosphere as the reactive gas, at a flow rate of 16 sccm (corresponding to a partial pressure value of 0.45 Pa). The films were prepared at room temperature, RT, conditions and the sputtering time was adjusted in order to keep an overall thickness close to 1 μm for all films. A plasma reactor (Zepto) was used to sputter-clean the substrates (glass ISO norm 8037-1 microscope slides, (100) p-type silicon wafers and Biaxial oriented Polyethylene Terephthalate (PET) from *Goodfellow*), using a pure Argon atmosphere at a RF power of 100 W applied for 900 s.

The morphology of the ZnO/Ag films were characterized by Scanning Electron Microscopy (SEM), using a NanoSEM - FEI Nova 200 (FEG/SEM) microscope, on fractured cross-section and top view conditions. The structure of the films was characterized by X-ray diffraction (XRD), using a Bruker D8 discover diffractometer (Co $\lambda_{K\alpha 1}$ =1.78897 Å), operating in a θ/2θ configuration. A step of 0.02° per 0.2 s and a 2θ angle ranging from 30 to 72° were selected.

In order to evaluate the piezoresistive properties of the ZnO/Ag films, the samples were subjected to a 4-point bending tests as described in [7], using a Shimadzu-AG-IS universal testing machine, with a load cell of 500 N. Before that, the electrical resistivity of the ZnO/Ag samples was determined by measuring the electrical current with a Keithley 487 picoammeter/voltage source during the applications of voltages ranging from -10 V to 10 V at a step of 1 V. The piezoelectric sensitivity of the ZnO/Ag samples was quantified by the gauge factor (*GF*), which is defined as the ratio between the variation of the relative electrical resistance and the mechanical deformation applied [19]:

$$GF = \frac{\Delta R/R_0}{\varepsilon} = \frac{\Delta \rho/\rho_0}{\varepsilon} + (1 + 2\upsilon) \quad (1)$$

In equation (1), R_0 is the steady-state material electrical resistance (in Ω) before deformation and ΔR is the resistance change (in Ω) caused by the mechanical deformation, ε. The change of resistance shows contributions from the geometric deformation $(1 + 2\upsilon)$, where υ is the Poisson ratio and from the relative electrical resistivity change $\left(\frac{\Delta\rho/\rho_0}{\varepsilon}\right)$. Ideally, the Poisson's value assumes the maximum value of 0.5, which means that the geometric effect contribution to the GF is 2.

3. Results and discussion

3.1. Morphological and structural characterization

A set of ZnO/Ag thin films was deposited with increasing Ag contents (obtained by varying the exposed Ag pellets area in the Zn target from 3 to 10 cm^2), with a fixed incident angle α = 45º to obtain zigzag nanostrutures. The SEM micrographs of as-deposeted samples are presented in Fig. 2.

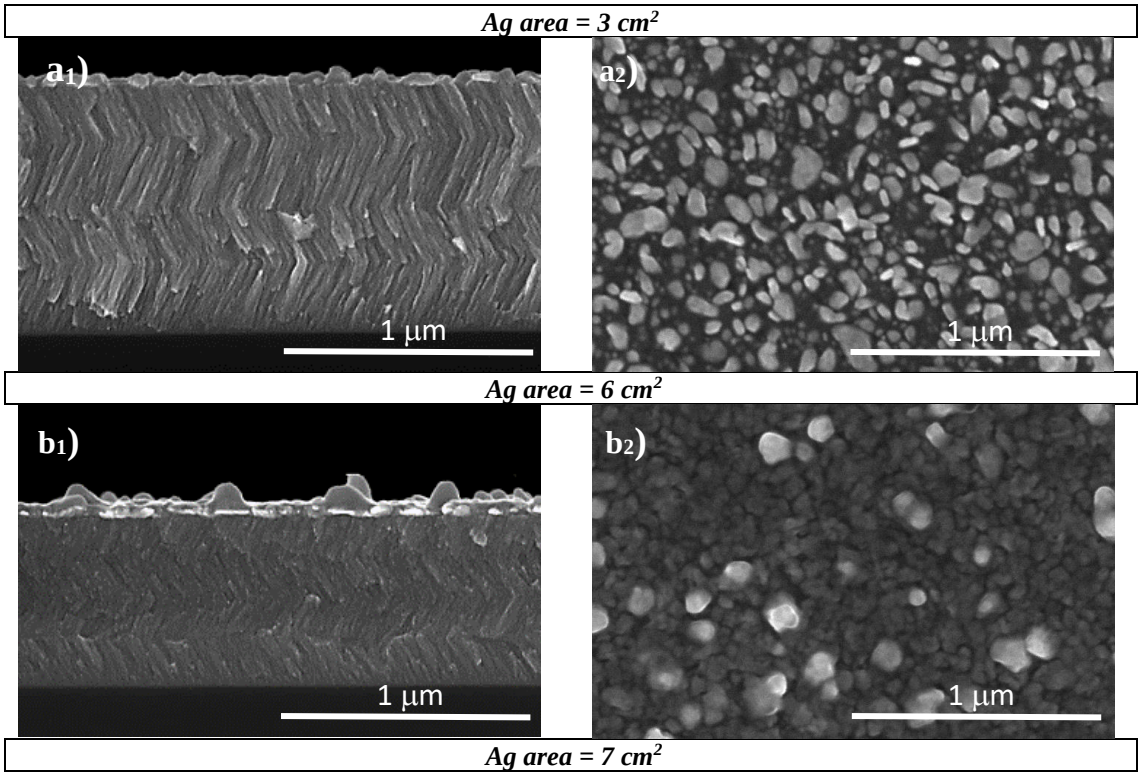

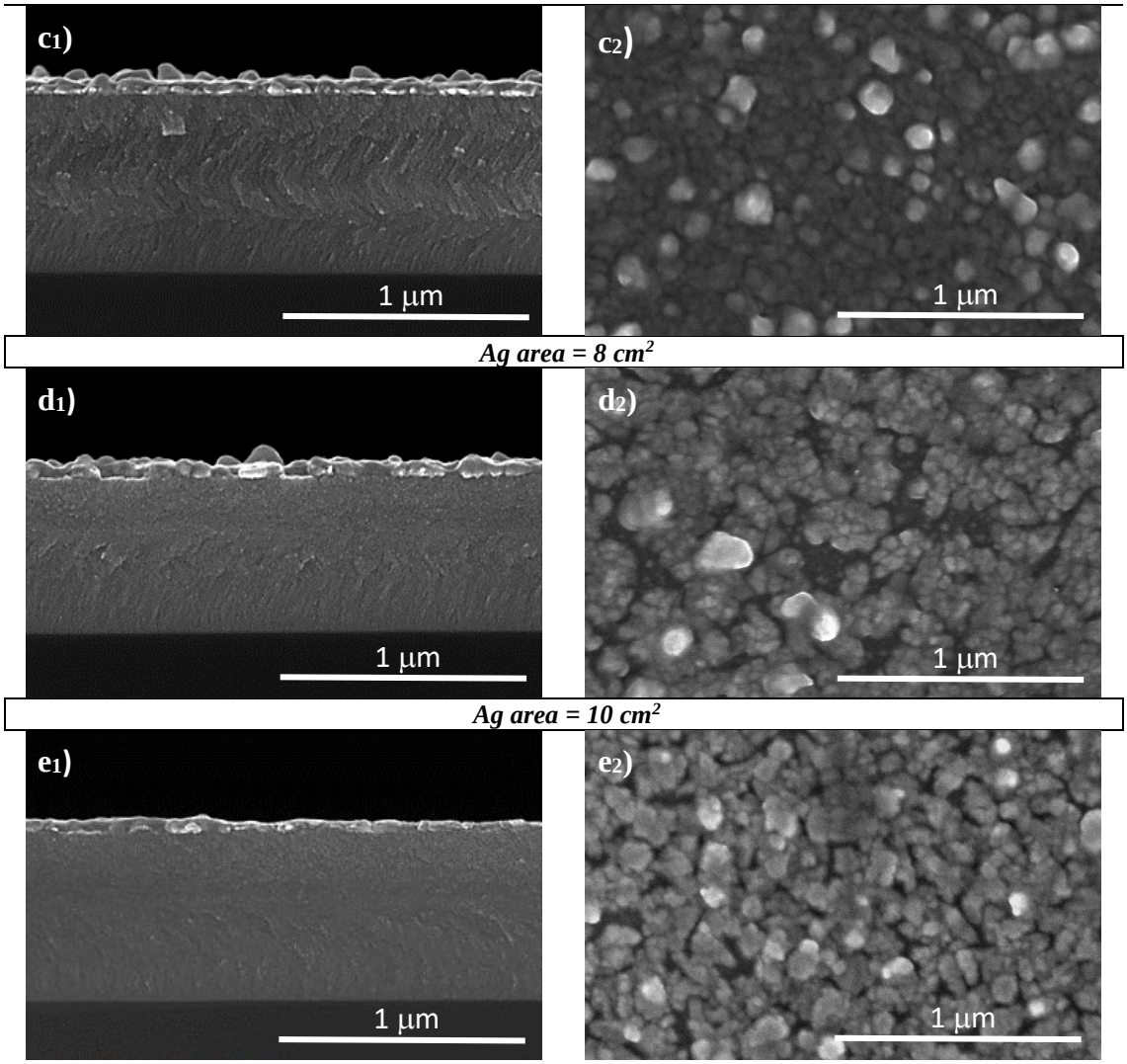

Figure 2. SEM cross-section and surface views of the ZnO-Ag thin films depositd on silico prepared using different concentrations of Ag.

From Fig. 2 (a_1 to e_1), it can be distinguish some zigzag morphological changes with increasing Ag content in the ZnO/Ag thin films. Thin and well-defined zigzags are observed in the ZnO/Ag thin film prepared with an Ag exposed area of 3 cm^2 (Fig. 4 a_1). This same sample reveals the highest average growth rate (50 nm min^{-1}). For the samples prepared with the highest Ag contents (Fig. 2 d_1 and e_1), the zigzag structure reduces dramatically, and the films seem to grow denser than the ones prepared with lower Ag contents (Fig. 2 a_1 to c_1). For intermediate Ag contents (Fig. 2 b_1 and c_1), the zigzag definition decreases sharply due to a steep decrease of the average growth rate (39 nm min^{-1}). The contribution of the Ag exposed area to the "co-deposition" process is then greatly increased and the zigzag columns become less defined. This tendency of the growth rate and undefined columns might be due to the lower sputtering yield

of ZnO [20] when compared to Ag [21]. As a general conclusion, it can be stated that Ag exposed areas below 6 cm^2 seem to be the best experimental conditions in order to obtain clear and well-defined zigzag structures in the ZnO/Ag "co-sputtered" films. Additionally, and as it can be observed in Fig. 2 (a_1 to e_1), increasing Ag contents leads to the formation of a small Ag layer at the top of the surface of the ZnO/Ag thin films, and some relatively large Ag nanoparticles start to appear close to the surface layer (Fig. 2 d_2 and e_2). This is expected since some small particles are evenly distributed along the columns due to the high Ag mobility and diffusion ability [22,23].

In order to check if these morphological changes were correlated with changes in the structural features, Fig. 3 shows the XRD patterns of the sputtered ZnO/Ag thin films. It is shown that pure ZnO films develop a polycrystalline hexagonal-like structure, as confirmed by the presence of dominant and very intense ZnO (002) and ZnO (101) diffraction peaks (ICSD database, card #01-070-8070), appearing at angular positions of $2\theta = 34.4^{o}$ and 36.2^{o}, respectively. By increasing Ag content in the films, the ZnO hexagonal (002) preferential growth, which is dominant in the ZnO film, is progressively changed by a (101) one for the films prepared within low exposed Ag area (3 cm^2), as it is observed by the low relative intensity of the diffraction peak located at $2\theta \approx 34.4^{o}$ (ZnO (002)). Furthermore, for intermediates exposed areas (6 and 7 cm^2), the hexagonal ZnO (101) growth almost disappears and the fcc-Ag (111) phase (card #04-0783) apprears, as evidenved by the (111) peak, located at $2\theta \approx 38.1^{o}$, this growth direction becoming the preferential one. Further, increasing even more the Ag content, the ZnO hexagonal (002) and (101) reveals a mixture of both diffraction growths and the fcc-Ag (111) phase remains the dominant one, which reveals a similar trend as previously observed for the nanostructure variations observed by SEM, Fig. 2 (a_1 to e_1).

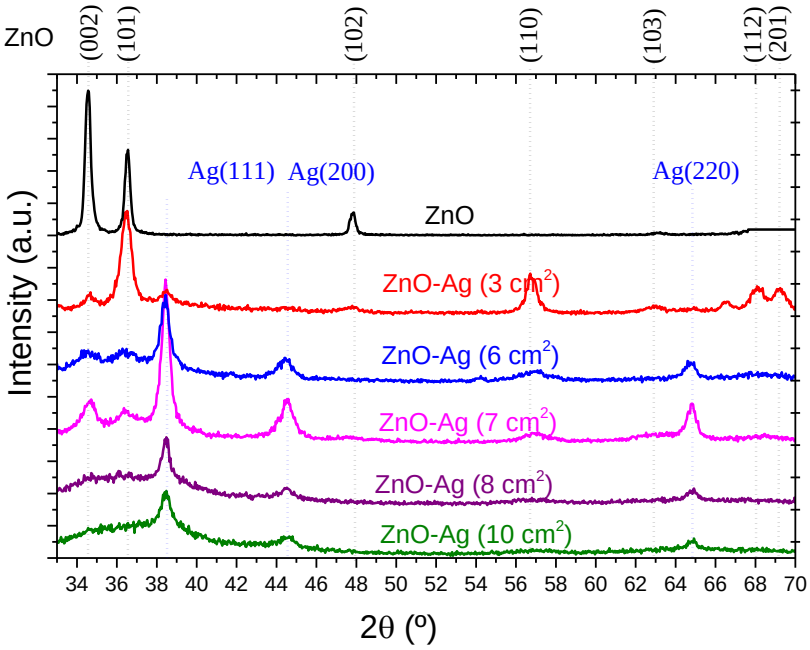

Figure 3. XRD diffractograms of the nanostructured ZnO/Ag thin films.

3.2 Electrical and electromechanical response

Fig. 4 shows the evolution of the room temperature electrical resistivity and the Ag concentration (at. %) as a function of the Ag exposed area on the Zn target surface.

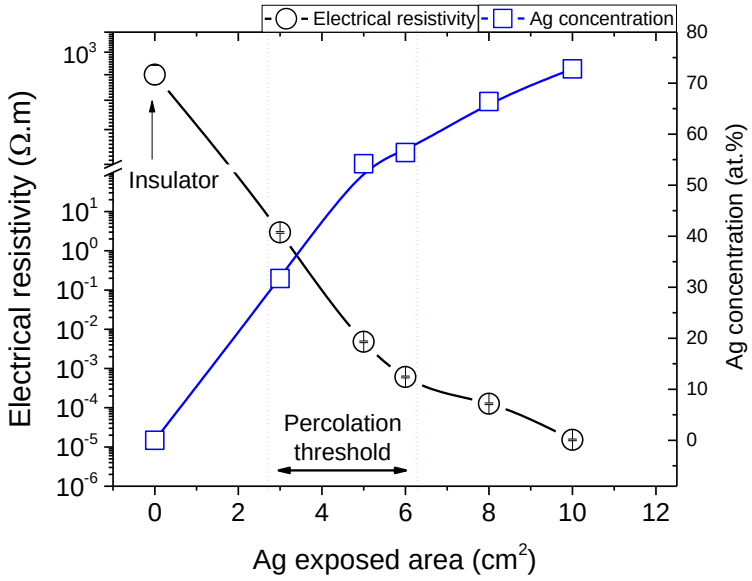

Figure 4. Room temperature electrical resistivity and Ag atomic concentration of as a function of the Ag exposed area.

As expected, the variation of the electrical resistivity of the ZnO/Ag thin films is mainly determined by the Ag concentration, the electrical resistivity decreasing with increasing Ag content in the samples (Figure 4), which results also in variations of the morphological and structural features, as previously analyzed (Figures 2 and 3). Several mechanisms have been proposed to explain the electron transport between separate metal islands, including tunnelling [24,25], space-charge limited current flow across the substrate surface, grain boundaries, vacancies, and surface effects [25], among others. Taking in account the existing theories, the results suggest that the decrease of the electrical resistivity is related to the decreasing distance between conductive Ag particles pairs, which influences the number of conductive paths and depends on the Ag concentration. The electrical resistivity decreases with the increase of the area of Ag pellets placed on the surface of the Zn target, as shown in Fig. 4. As a general trend, and considering the atomic composition of Ag in the thin films, ZnO/Ag samples exhibited higher resistivity values (2.95 Ω.m) for small amounts of Ag pellets, increasing Ag content, leads to a percolation threshold area, indicating the transition between states with long- and short-range connectivity between Ag particles, the electrical resistivity decreasing further to about 1.52×10^{-5} Ω.m for the highest Ag exposed area. It should be noted that this value is still significantly higher than that of bulk silver (1.5×10^{-8} Ω.m) which mainly originates, together with the lower Ag concentration, from the polycrystalline film growth with its grain boundaries, defects and surface roughness [26,27].

For sensing applications, both to quantify the electrical variation under bending and the ability of the electrical resistance to return to the initial value after and specific bending cycle are essential parameters. In order to quantify the piezoresistive response of the ZnO/Ag system, dynamic measurements were performed to determine the films' sensitivity, GF. Fig. 5 shows the variation of the electrical resistance ratio, $\Delta R/R_0$, as a function of time, for ZnO/Ag with 54

at.% Ag, with a z-deformation of 0.5 mm and velocity of 6 mm min^{-1}, during 40 cycles. The resuls are rerpesentative for the ones obained for the rest of the samples.

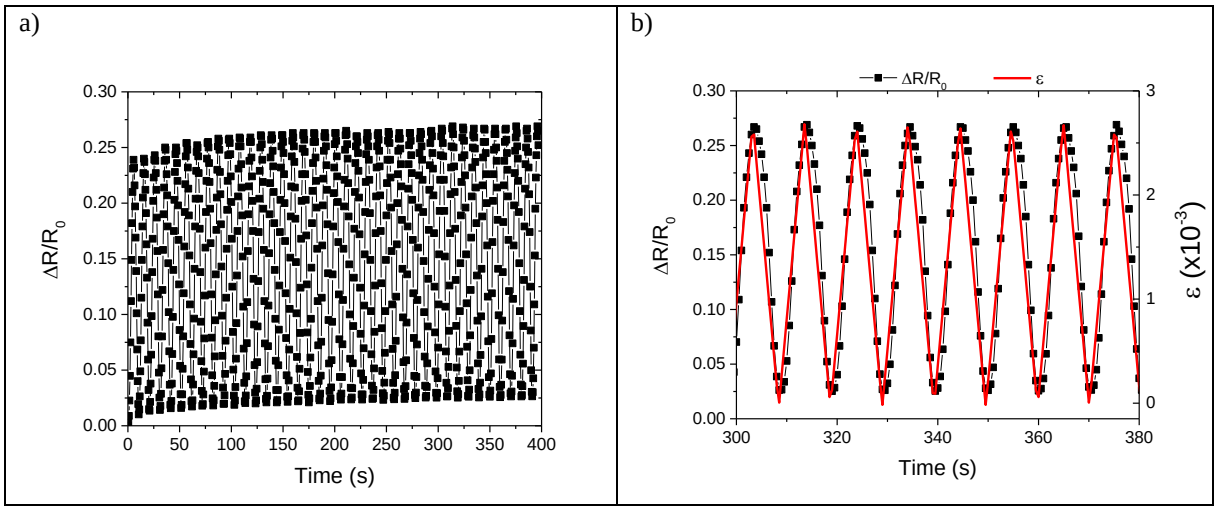

Figure 5. a) Electromechanical response after 40 bending cycles for the sample with 54 at.% of Ag with a z-deformation of 0.5 mm and deformation velocity of 6 $mm.min^{-1}$ b) Detail of the electromechanical response of the last cycles.

The main origin of the piezoresistive effect is the distribution of the conductive Ag particles within the ZnO matrix [28] (Fig. 4). Under mechanical solicitaion, the induced strain increases the distance between the conductive particles, enhancing the electrical resistivity of the thin films [29]. As illustrated in Fig. 5 a), the electrical resistance changes with the applied strain, and this trend is maintained for the different 40 cycles, showing a stable response with no aparent aging. Just some initial increase of the resistance is observed for the initial cycles related to stain relaxation of the as deposited films. Important to note is that after 40 cycles, the resistance remains unchanged (Fig. 5b). This is particularly relevant as when a metallic film deposited onto a polymeric substrate that is subsequently stretched, its electrical resistance R_0 increases under repeated cycling dur to micro-crack formation in the films [30].

Fig. 6 shows SEM micrographs taken on the surface of the ZnO/Ag films with 56 at.% Ag, deposited on PET substrates, after 40 cycles bending, showing large cavities and tracks, aligned along the surface of the samples, Fig. 6a).

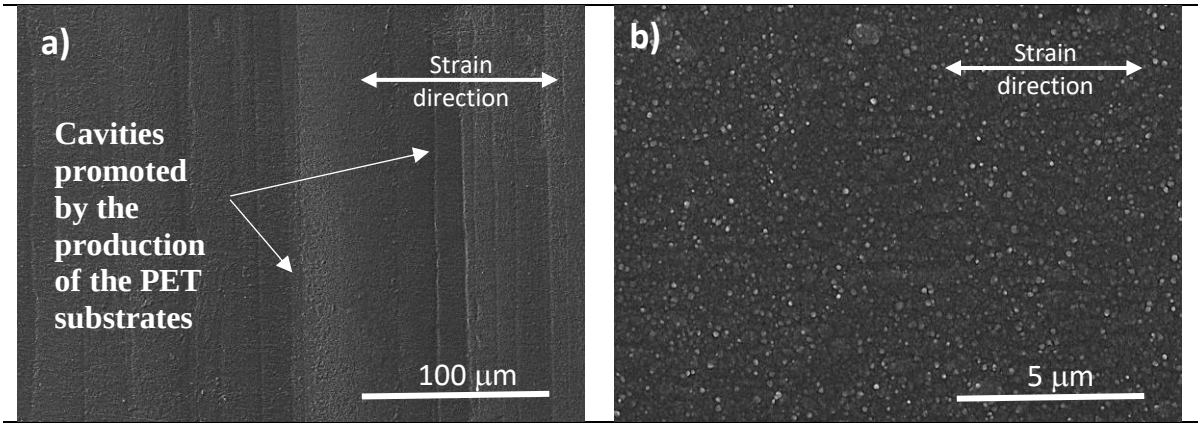

Figure 5. SEM micrographs of samples with 56 at. % Ag after bending with different magnifications, a) and b), measured on polymer substrates (PET).

The formation of cavities and tracks is intimately related to the presence of surface depressions or surface roughness, induced by the polymer substrate morphology. According to Smith *et al.* and Dong *et al.* [31,32], atoms being deposited in the neighbourhood of a surface cavity will be attracted by the sides of the surface cavity. As a result, the thin film grows aligned with the cavities and with the same orientation of the surface roughness. In our study, the cavities and tracks do not show any clear evidence of fracture along the strain direction (Fig. 6 a) and b)). As a result, it is concluded that the film deforms homogenously and the electrical resistivity is not affected by micro-cracks, showing the robustness and reliability of ZnO/Ag thin films for electromechanical applications.

The gauge factor for the different samples was obtaines from the linear fits of three different regions identified as low, intermediate and high applied deformations, Fig. 7.

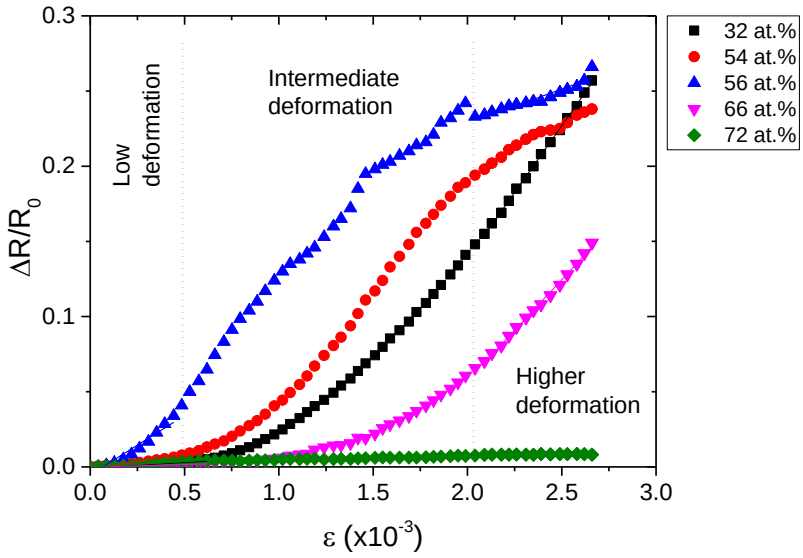

Figure 7. Relative resistivity variation, $\Delta R/R_0$, as a function of the longitudinal strain, ε, of the samples prepared with different amounts of Ag on PET substrates,

The slope of the linear fit, done according to Eq. 1, corresponds to the gauge factor of the sample. The results are presented in Table 1, each value of GF presented is the mean value measured in the last 4 cycles of the 40 cycles. The relative resistivity variation, $\Delta R/R_0$, as a function of the longitudinal strain, ε, indicates that the electrical resistivity variation of all samples increases with the applied deformation, but that it is non linear, the electrical resisriviry variation being larger as the deformation increases, Fig. 5 and Fig. 7. This trend will be discussed later in the text. As a general trend, the values of the gauge factor, Table 1, show a strong intrinsic contribution of the Ag to the sensitivity of the films, in particular for Ag concentrations below 66 at. %, and a negligible sensitivity for Ag concentrations above 66 at. %.

Table 1: Gauge factor values resulting of the linear fit of $\Delta R/R_0$ as function of stress for zigzag structures calculated inthe three different regions of deformation.

Ag (at. %)	$GF_{(Low)}$	$GF_{(Intermediate)}$	$GF_{(Higher)}$
32	8 ± 1	120 ± 3	177 ± 1
54	19 ± 1	122 ± 2	67± 3
56	78 ± 7	98 ± 4	45 ± 4
66	4 ± 1	64 ± 3	135 ± 2

72	8 ± 1	2.4 ± 0.1	0.8 ± 0.2

Increasing the deformation from low to intermediate values, the gauge factor changes from 8 ± 1 to 120 ± 3 for the sample with 32 at. % Ag, and this trend is maintained with increasing Ag content up to 66 at. %. For an amount of Ag of 72 at. %, the electrical resistivity is relatively low (1.52×10^{-5} Ω.m). Consequently, the contribution of Ag to the GF, for intermediate and higher deformations is only due to the geometric effects, Eq. 1. It is also found that the sample with a Ag content of 56 at.% is the most sensitive to the variation of applied strain. Moreover, it is observed that the region near 50 at.% of Ag at which the resistivity decreases heavily, Fig. 4, the percolation threshold zone is the region with the largest GF, Table 1. Considering as main explanation the creation or destruction of conductive paths and tunneling effect [24], one may suggest that $\Delta R/R_0$ increases/decreases under stretching due to the increased/decreased separation of conductive particles pairs, which influences the number of conductive paths, So, the three distinct stages, Fig. 7, are dominated by the variation of the distance of the conductive Ag particles under deformation, leading to variations of the tunneling distance. This mechanisms depends on Ag concentration and is associated with an electromechanical hysteresis (Figure 8) . After the first loading-unloading cycle, there is a competitive behavior between the destruction and reformation of conductive networks, Fig. 8 a), which tends to level off with increased number of cycles, Fig. 8 b).

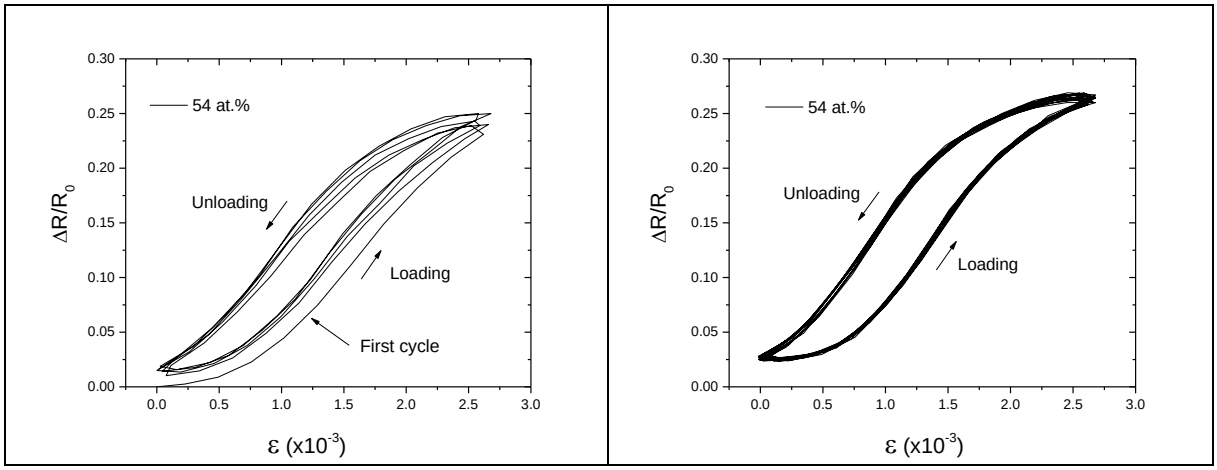

Figure 8. The relative resistivity variation, $\Delta R/R_0$, as a function of the longitudinal strain, ε, sample with 54 at. %. a) Electromechanical response for the first 5 bending cycles, b) for the last 20 bending cycles.

The repeated piezoresistive behavior of the ZnO/Ag thin films considered here can be entirely explained by the increment/reduction in the conductive particle's pairs distance along the strain direction. This is because $\Delta R/R_0$ increases when ε increases or vice versa. Consequently, within a complete loading and unloading cycle, the current can travel by tunneling effect through pairs of relatively neighbored Ag particles. The tunneling current between the step pairs is proportional to $Xd.\exp(-Xd)$ [33–35], where d is the average tunneling distance between adjacent steps, and X is the tunneling barrier height dependent function. According to the tunneling current expression, the resistance changes corresponding to the average tunneling distance d_0 and the strain ε is expressed as:

$$ln\frac{R}{R_0} = -\ln(1+\varepsilon) + Xd_0\varepsilon \quad (3)$$

and

$$X = \frac{2\pi}{h}\sqrt{2m\varphi} \quad (4)$$

where h is the Planck's constant, m is the mass of the charge carriers, and $\mathcal{J}$ is the tunneling barrier height [34,36].

The experimental results for electrical resistivity, give the percolation thresholds between 32 at.% and 56 at.% of Ag. These values are the critical filler fraction of Ag in the ZnO samples, at which the electrical response of the material suffers significant variations as a function of dopant concentration. Using Eq. 3 for the tunneling effect through conductive pairs, the values of d_0 as the tunneling distance were calculated and presented in Table 2.

Table 2: Calculated distances between two Ag particles for the different samples using the parameters derived from the fit with Eq. 3 and assuming a barrier height of 3 eV.

Ag (at.%)	$d_{0(Low)}$ *(nm)*	$d_{0\ (Intermediate)}$ *(nm)*	$d_{0\ (Hig)}$ *(nm)*
32	0.5	6.8	10.0
54	1.1	6.9	3.8
56	4.4	5.5	2.5
66	0.2	3.6	7.6
72	0.5	0.1	0.5

From the change of the Ag interparticle distance, it becomes possible to explain the behavior of the GF in the three different regions. For lower deformations, the distance between Ag particles is ~ 0.5 nm, for the sample with 32 at. %. Increasing stretching leads to increased separation of conductive particles pairs, from 0.5 to 10 nm, reducing the number of conductive paths and consequently increase the $\Delta R/R_0$ leading to higher GF's. These calculations demonstrate that increasing that tunneling distance strongly affects the GF of the ZnO/Ag system. Higher distances between Ag conductive particle pairs imply higher resistivities and consequently higher sensitivity of the transducers.

4. Conclusion

Zigzag-like ZnO/Ag thin films were prepared by GLAD, using a metallic Zn target with different amounts of Ag pellets, symmetrically distributed along the preferential erosion area. The change in the electrical resistivity of the ZnO/Ag thin films, due the increasing amount of Ag, induces strong variation of the response of the transducers due to their varying electrical

response, which contribute to the variation of the response of the piezoresistive ZnO/Ag system. The results show that the structure has a pronounced influence on the overall transducer response. Increasing the deformation from low to intermediate deformations, the gauge factors, increase from 8 ± 1, to 120 ± 3 for 32 at. % Ag. This trend is maintained with the increment of Ag content until 66 at. % Ag. After 40 bending cycles, the ZnO/Ag thin films do not show any clear evidence of fractures along the strain direction, which illustrates this ZnO/Ag thin film is very robust and reliable for sensing applications.

Acknowledgements

This work was supported by the Portuguese Foundation for Science and Technology (FCT) in the framework of the Strategic Funding UID/FIS/04650/2013 and project PTDC/EEI-SII/5582/2014. Armando Ferreira acknowledges the FCT for the SFRH/BPD/102402/2014 grant. Funding was also provided by the Region of Franche-Comté, the French RENATECH network. This work has also been supported by the EIPHI Graduate School (contract "ANR-17-EURE-0002"). Financial support from the Basque Government Industry Department under the ELKARTEK and HAZITEK programs is also acknowledged.

Bibliography

[1] A. Ferreira, V. Correia, E. Mendes, C. Lopes, J.F.V. Vaz, S. Lanceros-Mendez, Piezoresistive Polymer-Based Materials for Real-Time Assessment of the Stump/Socket Interface Pressure in Lower Limb Amputees, IEEE Sens. J. 17 (2017). doi:10.1109/JSEN.2017.2667717.

[2] X. Shuai, P. Zhu, W. Zeng, Y. Hu, X. Liang, Y. Zhang, R. Sun, C.P. Wong, Highly Sensitive Flexible Pressure Sensor Based on Silver Nanowires-Embedded Polydimethylsiloxane Electrode with Microarray Structure, ACS Appl. Mater. Interfaces. (2017). doi:10.1021/acsami.7b05753.

[3] N. Lu, D.-H. Kim, Flexible and Stretchable Electronics Paving the Way for Soft Robotics, Soft Robot. (2014). doi:10.1089/soro.2013.0005.

[4] A. Ferreira, S. Lanceros-Mendez, Piezoresistive response of spray-printed carbon nanotube/poly(vinylidene fluoride) composites, Compos. Part B Eng. 96 (2016). doi:10.1016/j.compositesb.2016.03.098.

[5] L. Arboleda, A. Ares, M.J. Abad, A. Ferreira, P. Costa, S. Lanceros-Mendez, Piezoresistive response of carbon nanotubes-polyamides composites processed by extrusion, J. Polym. Res. 20 (2013). doi:10.1007/s10965-013-0326-y.

[6] P. Costa, A. Ferreira, V. Sencadas, J.C. Viana, S. Lanceros-Méndez, Electro-mechanical properties of triblock copolymer styrene-butadiene- styrene/carbon nanotube composites for large deformation sensor applications, Sensors Actuators, A Phys. 201 (2013). doi:10.1016/j.sna.2013.08.007.
[7] A. Ferreira, J. Borges, C. Lopes, N. Martin, S. Lanceros-Mendez, F. Vaz, Piezoresistive response of nano-architectured TixCuy thin films for sensor applications, Sensors Actuators, A Phys. 247 (2016) 105–114. doi:10.1016/j.sna.2016.05.033.
[8] A. Kim, Y. Won, K. Woo, C.H. Kim, J. Moon, Highly Transparent Low Resistance ZnO / Ag Nanowire / ZnO Composite Electrode for Thin Film Solar Cells, ACS Nano. (2013). doi:10.1021/nn305491x Highly.
[9] P. Sheng, B. Abeles, Y. Arie, Hopping conductivity in granular metals, Phys. Rev. Lett. (1973). doi:10.1103/PhysRevLett.31.44.
[10] P. Smilauer, Thin metal films and percolation theory, Contemp. Phys. (1991). doi:10.1080/00107519108213805.
[11] P. Pedrosa, A. Ferreira, N. Martin, M. Arab Pour Yazdi, A. Billard, S. Lanceros-Méndez, F. Vaz, Nano-sculptured Janus-like TiAg thin films obliquely deposited by GLAD co-sputtering for temperature sensing, Nanotechnology. 29 (2018). doi:10.1088/1361-6528/aacba8.
[12] A. Ferreira, N. Martin, S. Lanceros-Méndez, F. Vaz, Tuning electrical resistivity anisotropy of ZnO thin films for resistive sensor applications, Thin Solid Films. 654 (2018). doi:10.1016/j.tsf.2018.03.090.
[13] A. Ferreira, J. Borges, C. Lopes, M.S. Rodrigues, S. Lanceros-Mendez, F. Vaz, Relationship between nano-architectured Ti1−xCux thin film and electrical resistivity for resistance temperature detectors, J. Mater. Sci. 52 (2017) 4878–4885. doi:10.1007/s10853-016-0722-x.
[14] A. Ferreira, C. Lopes, N. Martin, S. Lanceros-Méndez, F. Vaz, Nanostructured functional Ti-Ag electrodes for large deformation sensor applications, Sensors Actuators, A Phys. 220 (2014). doi:10.1016/j.sna.2014.09.031.
[15] M. Fahland, P. Karlsson, C. Charton, Low resisitivity transparent electrodes for displays on polymer substrates, Thin Solid Films. (2001). doi:10.1016/S0040-6090(01)01053-7.
[16] S.H. Cho, W.J. Lee, Effect of added metallic elements in Ag alloys on the durability against heat and humidity of indium zinc oxide/Ag alloy/indium zinc oxide transparent conductive multilayer system, Jpn. J. Appl. Phys. (2010). doi:10.1143/JJAP.49.111102.
[17] M. Arbab, Base layer effect on the d.c. conductivity and structure of direct current magnetron sputtered thin films of silver, Thin Solid Films. (2001). doi:10.1016/S0040-6090(00)01341-9.
[18] T.G. Knorr, R.W. Hoffman, Dependence of geometric magnetic anisotropy in thin iron films, Phys. Rev. 113 (1959) 1039–1046. doi:10.1103/PhysRev.113.1039.
[19] S. Beeby, G. Ensell, M. Kraft, N. White, MEMS mechanical sensors, Artech House, Boston, 2004.
[20] C.R. Aita, A.J. Purdes, K.L. Lad, P.D. Funkenbusch, The effect of O2 on reactively sputtered zinc oxide, J. Appl. Phys. (1980). doi:10.1063/1.327472.
[21] N. Maréchal, E. Quesnel, Y. Pauleau, Silver thin films deposited by magnetron sputtering, Thin Solid Films. (1994). doi:10.1016/0040-6090(94)90391-3.
[22] P. Pedrosa, E. Alves, N.P. Barradas, N. Martin, P. Fiedler, J. Haueisen, F. Vaz, C. Fonseca, Electrochemical behaviour of nanocomposite Agx:TiN thin films for dry biopotential electrodes, Electrochim. Acta. 125 (2014) 48–57. doi:10.1016/j.electacta.2014.01.082.
[23] J. Kulczyk-Malecka, P.J. Kelly, G. West, G.C.B. Clarke, J.A. Ridealgh, K.P. Almtoft, A.L. Greer, Z.H. Barber, Investigation of silver diffusion in TiO2/Ag/TiO2 coatings, Acta Mater. 66 (2014) 396–404. doi:10.1016/j.actamat.2013.11.030.

[24] C.W. Jiang, I.C. Ni, S. Der Tzeng, W. Kuo, Nearly isotropic piezoresistive response due to charge detour conduction in nanoparticle thin films, Sci. Rep. (2015). doi:10.1038/srep11939.
[25] G. Dittmer, Electrical conduction and electron emission of discontinuous thin films, Thin Solid Films. (1972). doi:10.1016/0040-6090(72)90122-8.
[26] K. Fuchs, The conductivity of thin metallic films according to the electron theory of metals, Math. Proc. Cambridge Philos. Soc. (1938). doi:10.1017/S0305004100019952.
[27] A.F. Mayadas, M. Shatzkes, Electrical-resistivity model for polycrystalline films: The case of arbitrary reflection at external surfaces, Phys. Rev. B. (1970). doi:10.1103/PhysRevB.1.1382.
[28] G.-Y. Huang, C.-Y. Wang, J.-T. Wang, First-principles study of diffusion of Li, Na, K and Ag in ZnO, J. Phys. Condens. Matter. (2009). doi:10.1088/0953-8984/21/34/345802.
[29] J. Lintymer, J. Gavoille, N. Martin, J. Takadoum, Glancing angle deposition to modify microstructure and properties of sputter deposited chromium thin films, Surf. Coatings Technol. (2003). doi:10.1016/S0257-8972(03)00413-4.
[30] O. Glushko, V.M. Marx, C. Kirchlechner, I. Zizak, M.J. Cordill, Recovery of electrical resistance in copper films on polyethylene terephthalate subjected to a tensile strain, Thin Solid Films. (2014). doi:10.1016/j.tsf.2013.12.055.
[31] L. Dong, R.W. Smith, D.J. Srolovitz, A two-dimensional molecular dynamics simulation of thin film growth by oblique deposition, J. Appl. Phys. 80 (1996) 5682–5690. doi:10.1063/1.363621.
[32] R. Smith, D. Srolovitz, Void formation during film growth: A molecular dynamics simulation study, J. Appl. Phys. (1996). doi:10.1063/1.360983.
[33] L. Chen, G.H. Chen, L. Lu, Piezoresistive Behavior Study on Finger-Sensing Silicone Rubber/Graphite Nanosheet Nanocomposites, Adv. Funct. Mater. 17 (2007) 898–904. doi:10.1002/adfm.200600519.
[34] A. Ferreira, M.T. Martínez, A. Ansón-Casaos, L.E. Gómez-Pineda, F. Vaz, S. Lanceros-Mendez, Relationship between electromechanical response and percolation threshold in carbon nanotube/poly(vinylidene fluoride) composites, Carbon N. Y. 61 (2013). doi:10.1016/j.carbon.2013.05.038.
[35] J. Zhao, C. He, R. Yang, Z. Shi, M. Cheng, W. Yang, G. Xie, D. Wang, D. Shi, G. Zhang, Ultra-sensitive strain sensors based on piezoresistive nanographene films, Appl. Phys. Lett. (2012). doi:10.1063/1.4742331.
[36] F.R. Al-Solamy, A.A. Al-Ghamdi, W.E. Mahmoud, Piezoresistive behavior of graphite nanoplatelets based rubber nanocomposites, Polym. Adv. Technol. (2012). doi:10.1002/pat.1902.